Restoration of Catalytic Activity beyond Wild-Type Level in Glucoamylase from *Aspergillus awamori* by Oxidation of the Glu400→Cys Catalytic-Base Mutant to Cysteinesulfinic Acid[†]

Henri-Pierre Fierobe,[‡] Ekaterina Mirgorodskaya,[§] Kirsten Arnvig McGuire,[‡] Peter Roepstorff,[§] Birte Svensson,*[,‡] and Anthony J. Clarke[||]

Department of Chemistry, Carlsberg Laboratory, Gamle Carlsberg Vej 10, DK-2500 Copenhagen Valby, Denmark, Department of Molecular Biology, Odense University, Campusvej 55, DK-5230 Odense M, Denmark, and Department of Microbiology, University of Guelph, Ontario N1G 2W1, Canada

Received September 8, 1997

ABSTRACT: Glucoamylase catalyzes the hydrolysis of glucosidic bonds with inversion of the anomeric configuration. Site-directed mutagenesis and three-dimensional structure determination of the glucoamylase from *Aspergillus awamori* previously identified Glu179 and Glu400 as the general acid and base catalyst, respectively. The average distance between the two carboxyl groups was measured to be 9.2 Å, which is typical for inverting glycosyl hydrolases. In the present study, this distance was increased by replacing the catalytic base Glu400 with cysteine which was then oxidized to cysteinesulfinic acid. Initially, this oxidation occurred during attempts to carboxyalkylate the Cys400 residue with iodoacetic acid, 3-iodopropionic acid, or 4-bromobutyric acid. However, endoproteinase Lys-C digestion of modified glucoamylase followed by high-pressure liquid chromatography in combination with matrix-assisted laser desorption ionization/time-of-flight mass spectrometry on purified peptide fragments demonstrated that all enzyme derivatives contained the cysteinesulfinic acid oxidation product of Cys400. Subsequently, it was demonstrated that treatment of Glu400→Cys glucoamylase with potassium iodide in the presence of bromine resulted in complete conversion to the cysteinesulfinic acid product. As expected, the catalytic base mutant Glu400→Cys glucoamylase had very low activity, i.e., 0.2% compared to wild-type. The oxidation of Cys400 to cysteinesulfinic acid, however, restored activity (k_{cat}) on α-1,4-linked substrates to levels up to 160% of the wild-type glucoamylase which corresponded to approximately a 700-fold increase in the k_{cat} of the Glu400→Cys mutant glucoamylase. Whereas Glu400→Cys glucoamylase was much less thermostable and more sensitive to guanidinium chloride than the wild-type enzyme, the oxidation to cysteinesulfinic acid was accompanied by partial recovery of the stability.

The hydrolysis of glycosidic bonds catalyzed by glycosyl hydrolases occurs via two distinct mechanisms leading to either retention or inversion of the anomeric configuration of the product (*1*). The three-dimensional structures of enzymes from about 25 glycosyl hydrolase structural families representing both categories have been solved over the past decade (for reviews, see *2*, *3*). These structures, in conjunction with mutational analysis and use of substrate analogues, provide excellent insight into characteristic features of the different catalytic machineries. Thus, the relative position of the "catalytic" water and the distance between the two catalytic groups were highlighted. The catalytic gap was generally 4.8−5.5 Å in the retaining enzymes as opposed to 9−10 Å in the inverting enzymes (*2*). Since the proton donor is located essentially at the same position relative to the bond to be cleaved in both mechanisms, the different span across the catalytic site reflects the location of the catalytic nucleophile and the catalytic base, respectively (Figure 1). In retaining enzymes, the nucleophile is near the substrate anomeric carbon at the bond to be cleaved, and, thus, substrate analogues with good leaving groups and high reactivity in the first step become covalently bound to the nucleophile (*4*, *5*); the second step consists of OH^- attack on C-1 promoted by the deprotonated acid catalyst acting as a catalytic base (Figure 1). With inverting enzymes, however, a water molecule that transfers OH^- in a nucleophilic reaction to C-1 of substrate (Figure 1) is situated between the substrate and the base catalyst (*2*).

The mechanistic difference between inverting and retaining enzymes implies strict requirement on the position of the nucleophile in the latter enzymes as opposed to flexibility for the position of the catalytic base in the inverting enzymes. Recently, it was confirmed for the retaining xylanase from

[†] H.-P.F. was supported by a Human Capital and Mobility fellowship (ERBCHBICT941224, EU) in 1995/1996. These studies were supported by grants from the Danish Biotechnology Program (95-02014) to B.S. and P.R., the EU Biotechnology Program (BIO2-CT94-3008) to B.S., and the National Science and Engineering Research Council of Canada (OGP3215) to A.J.C.

* Address correspondence to this author at the Department of Chemistry, Carlsberg Laboratory, DK-2500 Copenhagen Valby, Denmark. Telephone: + 45 33 27 53 45. Facsimile: + 45 33 27 47 08. E-mail: bis@crc.dk.

[‡] Carlsberg Laboratory.

[§] Odense University.

[||] University of Guelph.

S0006-2960(97)02231-9 CCC: $15.00
Published on Web 02/24/1998

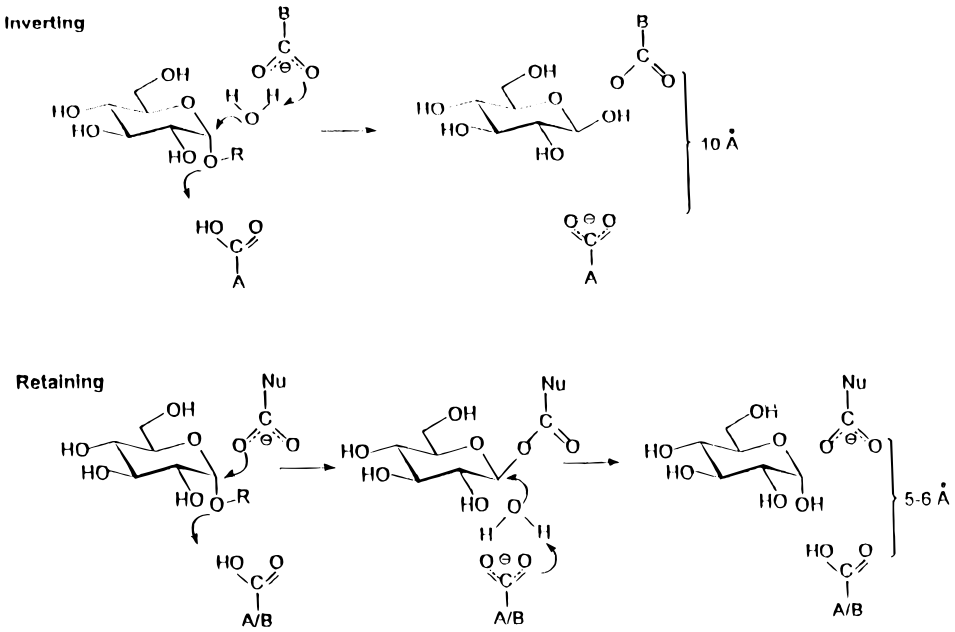

FIGURE 1: Schematic of the mechanisms of inverting and retaining glycosyl hydrolases. The general acid catalyst is at the bottom, and the base or the nucleophile at the top.

Bacillus circulans that the position of the nucleophile is very critical for activity (*6*). A small, approximately 1.6 Å, reduction of the distance between the catalytic groups by combination of mutagenesis and chemical modification of the nucleophile Glu78 caused 16−100-fold decrease in activity, whereas opening the gap by 1.6 Å more drastically resulted in [(1.5−5) × 10^3]-fold reduced activity (*6*).

We have been using the well-characterized glucoamylase (GA)[1]) from *Aspergillus awamori* as a model to study details of the catalytic mechanism of inverting enzymes. GA catalyzes the hydrolytic release of glucose from nonreducing ends of starch and related oligo- and polysaccharides, and cleaves α-1,6- in addition to α-1,4 glucosidic bonds, albeit with about 500-fold lower efficiency (*7*−*9*). The active site can accommodate seven consecutive glucose residues; cleavage occurs between subsites −1 and +1 (*10*−*12*). This 82 kDa enzyme contains an N-terminal catalytic domain (Ala1−Thr440), a Ser/Thr-rich, highly *O*-glycosylated linker (Ser441−Ser508), and a C-terminal starch binding domain (Cys509−Arg616) (*13*−*17*). The catalytic domain folds as a rare $(\alpha/\alpha)_6$ barrel, with six parallel inner and six outer α-helixes that run antiparallel to the inner ones (*18*), and the funnel-shaped active site created by the six α→α connecting segments comprises the best conserved regions in fungal GAs (*19*, *20*). Three-dimensional structures of GA from *A. awamori* var. *X100* in complex with 1-deoxynojirimycin (*21*) or two pseudotetrasaccharide inhibitors, acarbose (*22*) and D-*gluco*-dihydroacarbose (*23*), highlight the active site architecture and features of the inverting mechanism. The crystal structures in conjunction with mutational analysis identified Glu179 and Glu400 (Figure 2A) in the third and the sixth α→α segments as the general acid and base catalyst, respectively (*11*, *21*, *24*). The average distance of 9.2 Å measured between the two catalytic carboxyl groups (Table 1) is typical of inverting enzymes.

Table 1: Distances between Atoms in the Active Site of the Wild-Type Glucoamylase−Acarbose Complex and the Cys400-SO_2H Derivative

GA			distance (Å)
wild-type−acarbose[a]	Glu400 OE1	Glu179 OE1	7.39
	Glu400 OE1	Glu179 OE2	9.46
	Glu400 OE2	Glu179 OE1	8.97
	Glu400 OE2	Glu179 OE2	11.12
	Glu400 OE1	Acarb N4B	5.21
	Glu400 OE2	Acarb N4B	6.59
	Glu400 OE1	Acarb C1A	3.94
	Glu400 OE2	Acarb C1A	5.56
Cys400-SO_2H[b]	Cys400 SO1	Glu179 OE1	8.65
	Cys400 SO1	Glu179 OE2	10.73
	Cys400 SO2	Glu179 OE1	10.22
	Cys400 SO2	Glu179 OE2	12.17

[a] Crystal structure (*22*). [b] Distances deduced from the computer-generated model (see Figure 2B).

The impact of the location of the catalytic base on mechanism and activity was studied by chemical modification of the catalytic base mutant Glu400→Cys of *A. awamori* GA. The catalytic domain contains three disulfide bridges and one free thiol group, Cys320. The latter residue reacts with 5,5′-dithiobis(2-nitrobenzoic acid) (Ellman's reagent) only after denaturation (*9*), but to avoid any possible reaction of this cysteine, a double mutant GA (Cys400 GA)[1] was generated comprising both Glu400→Cys and Cys320→Ala. The Cys320→Ala GA retains both wild-type stability and activity (*9*) as expressed in *Pichia pastoris*, a host recently demonstrated to be efficient for overproduction and secretion of authentic GA (*25*). The present paper describes experiments originally designed to carboxalkylate the catalytic base mutant Cys400 GA with iodoacetic, 3-iodopropionic, or 4-bromobutyric acid, but MALDI MS peptide mapping of the obtained GA derivatives led to the identification of the

[1] Abbreviations: GA, glucoamylase; Cys400 GA, Cys320→Ala/Glu400→Cys glucoamylase; Cys400-SO_2H GA, cysteinesulfinic acid at Cys400 in Cys320→Ala/Glu400→Cys glucoamylase; DP, degree of polymerization; DTT, dithiothreitol; G2, maltose; G7, maltoheptaose; GdnHCl, guanidine hydrochloride; MALDI MS, matrix-assisted laser desorption ionization mass spectrometry; PNGaseF, peptide-*N*-glycosidase; TFA, trifluoroacetic acid.

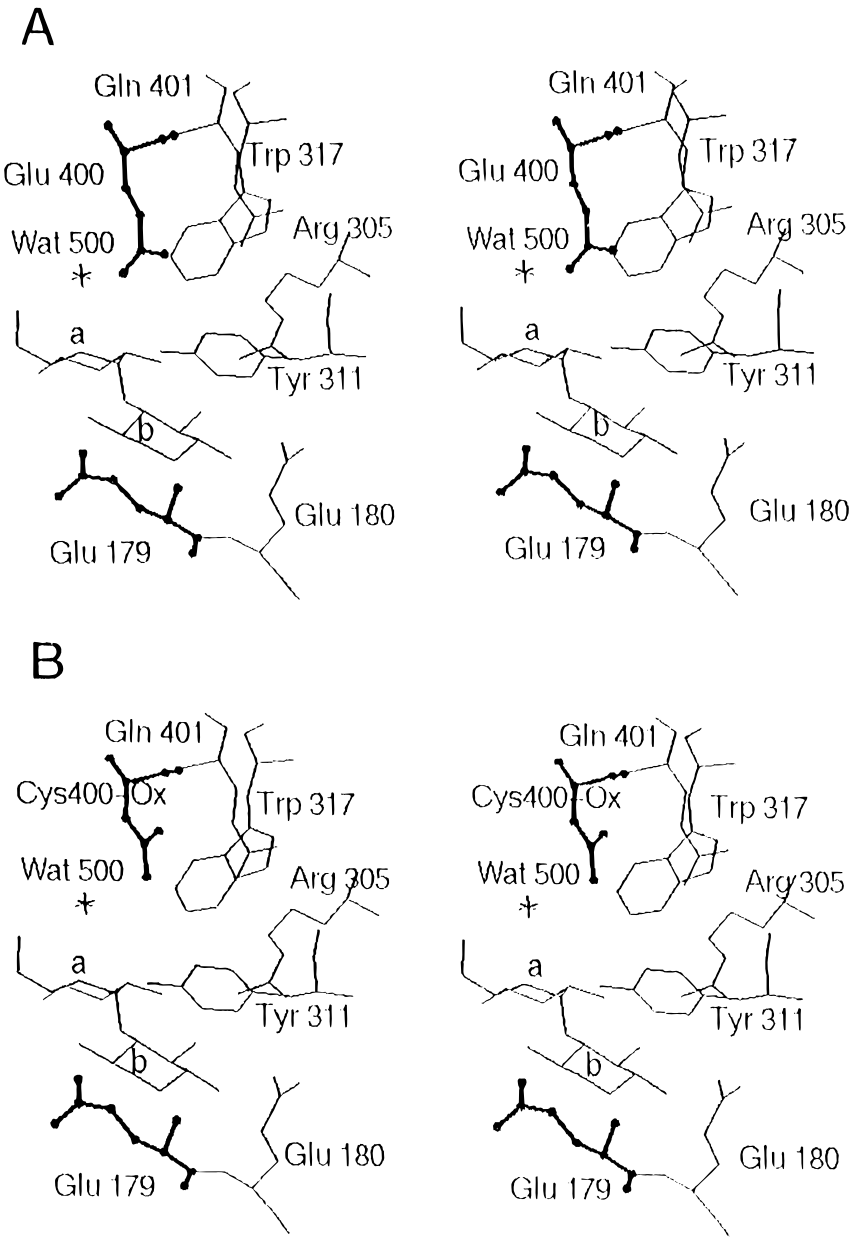

FIGURE 2: Stereoview of the active site of (A) *A. awamori* var. *X100* GA (*22*) in complex with pseudotetrasaccharide acarbose; only rings a (left) and b (right) of acarbose are shown. (B) The same view designed by computer simulation of the Cys400-SO_2H GA derivative. The side chains at position 400 (the catalytic base) and of the general acid catalyst Glu179 are in boldface type.

cysteinesulfinic acid derivative of Cys400. Reaction conditions are then described for the specific oxidation of the Cys400 thiol to sulfinic acid by potassium iodide in the presence of bromine which yields a highly active GA derivative. To our knowledge the results are the first report of a cysteinesulfinic acid directly participating in the catalytic mechanism of an enzyme.

MATERIALS AND METHODS

Reagents and Substrates. Maltoheptaose, the glucose oxidase kit, α-cyano-4-hydroxycinnamic acid, 5,5′-dithiobis-(2-nitrobenzoic acid) (Ellman's reagent), dithiothreitol (DTT), DPCC-trypsin, and *n*-octyl β-D-glucopyranoside were from Sigma (St. Louis, MO), and maltose monohydrate and potassium iodide were from Merck (Darmstadt, Germany). Guanidine hydrochloride (GdnHCl) was from Fluka (Buchs, Switzerland). Iodoacetic acid, 3-iodopropionic acid, 4-bromobutyric acid, 2,5-dihydroxybenzoic acid, and 2-hydroxy-5-methoxybenzoic acid were purchased from Aldrich (Steinheim, Germany), while Amersham provided iodo[2-^{3}H]acetic acid (sp. act. 205 mCi/mmol). Acarbose was a generous gift of Drs. D. Schmidt and E. Truscheit, Bayer AG (Wuppertal, Germany). Acarbose−Sepharose was prepared essentially as described (*26*). Endoproteinase Lys-C and peptide-*N*-glycosidase (PNGase F) were purchased from Boehringer Mannheim Scandinavia (Kvistgård, Denmark), while Sequazyme C-Peptide Sequencing Kit was a product of PerSeptive Biosystems Inc. (Framingham, MA).

Strains and Plasmids. *Pichia pastoris* GS115 (*HIS4*$^-$) was from Invitrogen (San Diego, CA). Transformation of *P. pastoris* and selection of clones that overexpress wild-type and Cys320→Ala/Glu400→Cys GA encoding cDNAs were previously described (*25*). Briefly, a DNA fragment containing the GA cDNA and the reporter gene *HIS4* was

inserted into the host genome by recombination to replace an alcohol oxidase gene (*AOX1*) downstream of a strong, methanol-inducible promotor. Transformants harboring the GA-encoding cDNA insert were identified using a double selection for ability to grow in the absence of histidine, and failure to grow with methanol as carbon source.

Expression and Purification of Wild-Type and Mutant GAs. *P. pastoris* transformants were grown in BMGY (13.4 g/L Yeast Nitrogen Base without amino acids, 20 g/L peptone, yeast 10 g/L extract, 1% glycerol, 0.4 mg/L biotin, and 0.1 M potassium phosphate, pH 6; 5 × 1 L in 5 L flasks) until an OD_{600} of 25. The cells were harvested by centrifugation at room temperature for 10 min (3000*g*) and resuspended in BMMY (13.4 g/L Yeast Nitrogen Base without amino acids, 20 g/L peptone, 10 g/L yeast extract, methanol ranging from 0.75%, 0.4 mg/L biotin, and 0.1 M potassium phosphate, pH 6; 2 × 0.5 L in 5 L flasks) to induce production of GA. After 48 h, the culture was centrifuged and the supernatant containing GA stored at 4 °C. The pellet was incubated in BMMY and the supernatant collected as above. The first and second supernatants were combined, concentrated to 300 mL (Pellicon cell; Amicon membrane, cutoff 10 kDa), applied to DEAE-Sepharose 650 M (Pharmacia, Uppsala, Sweden; 2.5 × 10 cm; equilibrated in 25 mM sodium phosphate pH 7.0), and eluted by a linear gradient from 0 to 0.4 M NaCl (2 × 500 mL). Fractions containing GA were combined, and the enzyme was purified by affinity chromatography on acarbose−Sepharose (1.1 × 10 cm) in 0.1 M sodium acetate, pH 4.5, 0.5 M NaCl. The GA was eluted with 1.7 M Tris·HCl, pH 7.6 (*26*), and checked by SDS−PAGE (12.5%) after dialysis. In *P. pastoris*, only the G1 form (*13*, *14*) of recombinant GA was produced (*25*). GA concentrations were determined either by amino acid analysis (*27*), spectrophotometrically using $\epsilon_{280} = 1.37 \times 10^5$ $M^{-1}\cdot cm^{-1}$ (*27*), or by fourth-derivative spectroscopy (*28*) using a Perkin-Elmer Lambda 9 UV/VIS Spectrometer (Bodenseewerk, Perkin-Elmer GmbH, Ueberlingen, Germany).

Fluorometric Titration. Fluorescence spectra were measured with a Perkin-Elmer LS50 Luminescence spectrometer at 25 °C with λ_{ex} set at 280 nm. Fluorometric titration of Cys400 GA in 50 mM sodium acetate buffer, pH 4.6, with maltose (0−12.3 mM) and subsequent determination of K_d and ΔF% values were performed as previously described (*27*).

Chemical Modifications. Cys400 GA was treated with 0.2 M iodoacetic acid, 0.1 M 3-iodopropionic acid, or 0.12 M 4-bromobutyric acid in 0.5 M sodium acetate (10−50 mL) at 25 °C for 20 h (pH 4.5), 16 h (pH 4.5), and 15 h (pH 5.1), at final enzyme concentrations of 43 μM, 12.7 μM, and 5.5 μM, respectively. KI was added to 0.5 M in the reaction with 4-bromobutyric acid. The reactions were stopped by dilution with 50 mM sodium acetate pH 4.5 (20 volumes), followed by dialysis for 3 h at room temperature and 16 h at 4 °C against 5 and 15 L, respectively, of the same buffer. The treatment with 4-bromobutyric acid/KI and subsequent quenching and dialysis were repeated once as described above. The resulting Cys400 GA derivatives were concentrated to 3−10 mL (Amicon cell, membrane cutoff 20 kDa) to give a final enzyme concentration of 7−30 μM, aliquoted, and stored at −20 °C. Cys400 GA (48.8 μM) was also treated with 0.2 M iodo[2-^{3}H]acetic acid (0.5 mCi) as above (final volume, 500 μL). The reaction mixture was diluted with 750 μL of 50 mM sodium acetate, pH 4.5, and dialyzed against the same buffer at 4 °C (3 × 2.5 L, 24 h). The incorporation stoichiometry was assessed by scintillation counting (samples adsorbed on glass fiber filters using a Beckman, LS 6000IC, and Ecoscint O from National Diagnostics, Atlanta, GA) and determination of protein concentration by amino acid analysis. During the preparative chemical modifications, aliquots (100−500 μL) were removed at specific intervals to monitor both the decrease in thiol content and the increase in activity toward maltoheptaose (see below).

Oxidation of Cys400 GA (3.1 μM, final concentration) in 0.2 M sodium acetate buffer, pH 5.1 at 25 °C, was done by mixtures of 8 μM−2 mM Br_2 and 0.4−2 M KI for up to 96 h. At specific intervals of time, 25 μL samples of the reaction mixtures were withdrawn and assayed for activity against maltose (see below). In semipreparative scale oxidations, 1.25−2.5 mL of 3.1 μM Cys400 GA in 0.2 M sodium acetate buffer, pH 5.1, was treated with 10.4 μM Br_2 and 0.8 M KI. After incubation at 25 °C for 84 h, the reaction mixtures were subjected to dialysis against Milli-Q water (3 × 2 L) at 4 °C over 24 h, and then freeze-dried.

Thiol Group Analysis. Wild-type GA and the various GA derivatives (2−5 nmol) were incubated in 0.2 mM 5,5′-dithiobis(2-nitrobenzoic acid), 6 M GdnHCl, 50 mM Tris, pH 8 (final volume, 100 μL). After 15 min, the absorbance was measured at 412 nm (*29*) in microcuvettes. The thiol concentration was calculated from $\epsilon_M = 13\,700$ $M^{-1}\cdot cm^{-1}$ for the liberated 2-nitrothiobenzoate anion. The extinction coefficient was confirmed by establishing a standard curve for cysteine (0−30 μM) under the same conditions.

Peptide Mapping. Samples of GA derivatives (approximately 2 nmol) were digested with 1 μg of endoproteinase Lys-C in 100 μL of 50 mM ammonium bicarbonate buffer, pH 7.8, containing 10 mM octyl glucoside at 37 °C for 18 h. Half of the digests was directly subjected to reverse-phase HPLC on a 4 mm × 250 mm Nucleosil C_{18} column (300 nm pore size, 10 μm particle size) at 45 °C. The equilibration buffer was 0.1% trifluoroacetic acid (TFA), and the peptides were eluted at a flow rate of 1 mL/min by the application of a nonlinear gradient over 50 min to 90% CH_3-CN in 0.08% TFA. The column eluates were monitored at 214 nm, and separated peptides were collected manually for MALDI MS analysis (see below). The second half of the digests was treated with 130 mM DTT (final concentration) for 30 min at 37 °C prior to separation by HPLC. In some cases, isolated peptides were dissolved in 20 μL of 50 mM sodium phosphate buffer, pH 7.4, and enzymatically deglycosylated using 0.5 unit of PNGaseF at 37 °C for 18 h. This deglycosylation of N-linked carbohydrate chains facilitated analysis by MALDI MS. In another experiment, selected tryptic peptides from the GA derivative prepared using iodo-[2-^{3}H]acetic acid (see above) were purified, following prior reduction and alkylation with 2-vinylpyridine, by a combination of Sephadex G100 gel filtration and reverse-phase HPLC on a C_{18} column (Vydac #218TP54) essentially as previously described (*13*, *30*).

Carboxypeptidase Y digestion of deglycosylated peptides was performed employing the Sequazyme C-Peptide Sequencing Kit as per manufacturer's instructions (PerSeptive

Table 2: Kinetic Parameters for the Hydrolysis of Maltose and Maltoheptaose by Wild-Type, Cys400, and Cys400-SO_2H GAs[a]

	maltose			maltoheptaose		
enzyme	k_{cat} (s^{-1})	K_m (mM)	k_{cat}/K_m (s^{-1} mM^{-1})	k_{cat} (s^{-1})	K_m (mM)	k_{cat}/K_m (s^{-1} mM^{-1})
wild-type	6.8 ± 0.11[b]	3.0 ± 0.13	2.3 ± 0.11	54 ± 0.8	0.12 ± 0.01	443 ± 30
Cys400	$0.015 \pm 2 \times 10^{-4}$	2.7 ± 0.13	$0.0055 \pm 3 \times 10^{-4}$	0.12 ± 0.002	0.45 ± 0.02	0.26 ± 0.012
Cys400-SO_2H	10.4 ± 0.01	2.5 ± 0.02	4.2 ± 0.03	86 ± 0.8	0.45 ± 0.01	191 ± 5

[a] Determined at 45 °C in 50 mM sodium acetate, pH 4.5. [b] Standard deviation.

Biosystem Inc.). The products of this carboxypeptidase digestion were identified by MALDI MS analysis.

MALDI MS. Mass spectrometric analyses of proteins and peptides were acquired on a Voyager-Elite time-of-flight MALDI mass spectrometer (PerSeptive Biosystem Inc.) (*31*) as previously descibed (*25*). Briefly, a 9:1 mixture of 25 g/L 2,5-dihydroxybenzoic acid and 25 g/L 2-hydroxy-5-methoxybenzoic acid in 0.1% TFA/33% CH_3CN was used as the matrix for protein samples, whereas the matrix for peptides was 20 g/L α-cyano-4-hydroxycinnamic acid in 70% CH_3CN. All mass spectra were obtained in the linear mode using delayed extraction and calibrated using appropriate external standards. Sample preparation involved placing 1 μL of a sample solution on a probe tip followed by 1 μL of the appropriate matrix and drying in air. Data processing was performed using the program GRAMS/386 (Galactic Industries Corp.).

Enzyme Kinetics. Initial rates of hydrolysis were determined at 45 °C in 50 mM sodium acetate, pH 4.5, using up to 15 concentrations [$(0.1-8)K_m$] of maltose and maltoheptaose. Enzyme concentrations were 2.5−70 nM for wild-type GA, 1.1−19 μM for Cys400 GA, and 2−70 nM for Cys400-SO_2H GA. Glucose was quantified by the glucose oxidase method (*24*, *32*, *33*) monitored in microtiter plates using a CERES UV900 Scanning Autoreader (Bio-Tek Instruments, Inc., Winooski, VT). Values of k_{cat} and K_m were obtained from plots of initial rates, v, versus v/[S] according to the Michaelis−Menten equation by using the ENZFITTER program (*34*). Standard deviations of k_{cat} and K_m in Table 2 were determined from the plots using the same program.

Isoelectric Focusing. Isoelectric focusing (pH 3.5−5.5) of wild-type and Cys400 GA derivatives was conducted using the Phast-System (Pharmacia) according to the manufacturer's instructions.

Thermostability. Wild-type GA, Cys400 GA, or Cys400-SO_2H GA (0.6 μM) in 0.1 M sodium acetate, pH 4.5, was incubated at varying temperatures (20−85 °C) for 5 min and then immediately frozen in an alcohol bath at −80 °C. After thawing, the residual activity was measured toward 70 mM maltose essentially as above. T_{50} was defined as the temperature corresponding to loss of 50% of the initial activity.

Guanidine Hydrochloride Denaturation. Wild-type GA, Cys400 GA, or Cys400-SO_2H GA (0.25 μM) was incubated for 1 h at room temperature with varying concentrations (0−7.7 M) of GdnHCl in 50 mM sodium acetate, pH 4.5, using a previously decribed procedure (*35*). Protein unfolding was monitored by the decrease in fluorescence (excitation at 280 nm and emission at 320 nm) using a Perkin-Elmer LS50 luminescence spectrometer. The fraction of unfolded enzyme, f_u, was calculated using the equation: $f_u = (F_N - F_{obs})/(F_N - F_{obs})$ where F_N and F_U are the fluorescence intensities recorded for the native and the unfolded protein, respectively, and F_{obs} is the fluorescence observed at a given concentration of GdnHCl. Standard free energy parameters were not calculated, since the unfolding of GA is not reversible (*16*).

Molecular Simulation. Using the coordinates (PDB accession code 1AGM) of the wild-type GA−acarbose complex (*22*), the substitution Glu400→Cys and the oxidation to Cys400-SO_2H were simulated by aid of the program Insight II 95.0 (Biosym, San Diego, CA). The φ and ψ angles of the Glu400 residue were maintained in the two derivatives, and the resulting structures were checked for steric interference. Finally, distances in the active site of the generated models were measured using the same program.

RESULTS

Design, Production, and Ligand Binding of Cys400 GA. Glu400→Cys was introduced in Cys320→Ala GA, and the double mutant (identified as Cys400 GA) was produced in the methylotrophic yeast *P. pastoris* (*25*). This strategy was chosen to preclude the possible modification/oxidation of Cys320 present in wild-type GA at the high reagent concentrations used in the various reactions. The Cys320→Ala mutation was previously shown to have no significant effect on stability or enzymatic activity (*9*). Recombinant wild-type GA and Cys400 GA were both obtained in yields of 0.2−0.4 g/L of *P. pastoris* supernatant without adverse posttranslational modification (*25*).

Cys400 GA had only 0.2% activity of wild-type GA toward either maltose or maltoheptaose, and as the K_m values remained unchanged and increased 3.5-fold, respectively, the catalytic efficiency of the enzyme was similarly reduced (Table 2). As with the K_m, the K_d value of Cys400 GA for maltose remained unchanged at 1.09 mM compared to the wild-type GA (*27*) as determined by fluorometric titration. The ΔF% value, equal to 20.7%, was also as for wild-type GA (*27*). These unchanged values of K_m and K_d indicated that replacement of the wild-type catalytic nucleophile Glu400 with Cys did not significantly alter the conformational characteristics of the active site in Cys400 GA and that the Cys400 residue was not engaged in disulfide bond formation or otherwise conjugated to a group of substantial size.

Modification of Cys400 GA with Haloalkylcarboxylic Acids. Initial experiments with Cys400 GA pertained to chemical modifications involving carboxyalkylation (see Materials and Methods) with intent to decrease the distance between the two catalytic carboxyl groups of the Glu residues 179 and 400 in wild-type GA. The progress of the reaction was monitored by both the restoration of activity toward 70 mM maltoheptaose (Figure 3A) and the loss of the sole free sulfhydryl in Cys400 GA by titration with Ellman's reagent (Figure 3B). The restored activity was directly proportional

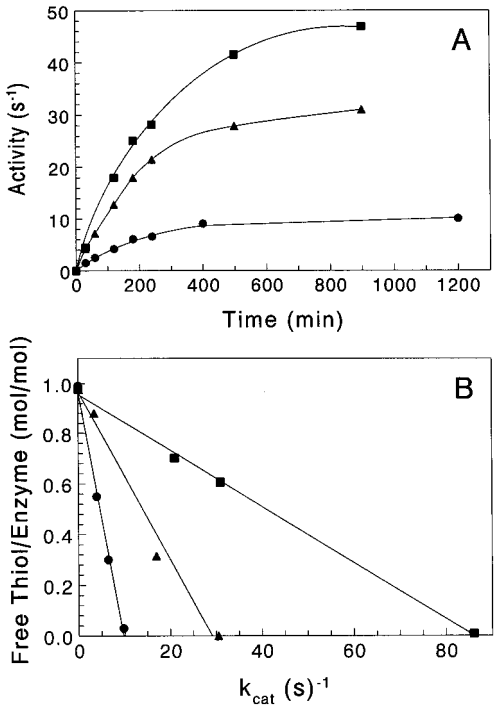

FIGURE 3: (A) Restoration of activity in Cys400 GA following treatment with haloalkylcarboxylic acids. The activity (k_{cat}, s^{-1}) toward maltoheptaose (70 mM; i.e., saturating concentration) was monitored at the times indicated for Cys400 GA treated with 0.2 M iodoacetic (●), 0.1 M iodopropanoic (▲), and 0.12 M bromobutyric (■) acids. For bromobutyric acid, only the first incubation is shown (15 h); a second incubation (see Materials and Methods) results in an activity of 87 s^{-1}. (B) Correlation of the residual thiol content of Cys400 GA and activity toward maltoheptaose (70 mM, i.e., saturating concentration) during chemical modification with 0.2 M iodoacetic (●), 0.1 M iodopropanoic (▲), and 0.12 M bromobutyric (■) acids.

to the loss of the thiol content. Control experiments with wild-type GA and alkylating reagents, or Cys400 GA without added reagent, indicated that the reaction conditions did not affect the activity. Cys400 GA treated with iodoacetic acid, iodopropanoic acid, and bromobutyric acid (see Materials and Methods) had k_{cat} values of 20%, 60%, and 160% of wild-type, respectively. However, peptide mapping of Cys400 GA treated with iodo[2-^{3}H]acetic acid and MALDI MS of the radiolabeled peptide revealed alkylation of only His254 in approximately 50% yield. This residue is far from the active site of GA (*18*), and was previously shown to undergo carboxymethylation without affecting activity (*36*). Accordingly, no significant overalkylation was detected by MALDI MS analysis since the wild-type (*25*), Cys400 GA, and Cys400 GA treated with iodoacetic acid all gave a very broad peak (reflecting the glucan heterogeneity of GA) centered around a mass of 82.3 kDa.

Peptide maps were made of endoproteinase Lys-C digests of Cys400 before (Figure 4A) and after (Figure 4B) attempts to alkylate (see Materials and Methods). The Thr379−Lys404 peptide fragment was isolated and identified by MALDI MS which confirmed that Cys400 was not alkylated with any of the haloalkylcarboxylic acids. However, two forms of Thr379−Lys404 with average masses of 2767 and 2799 Da were isolated from the Cys400 GA derivatives after release of the N-linked carbohydrate chain at Asn395 using PNGaseF. The former corresponded to the calculated average mass (2767 Da) of the Thr379−Lys404 sequence

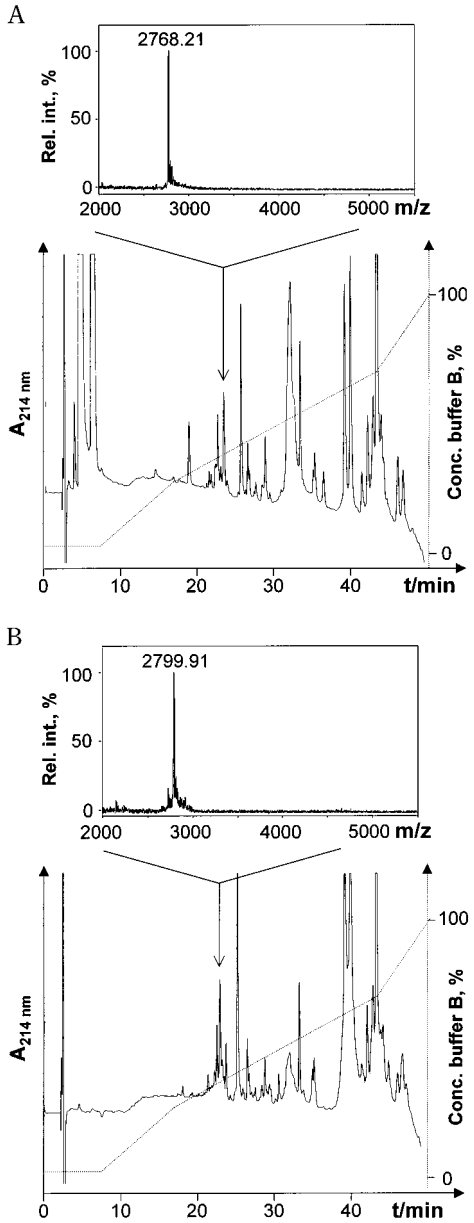

FIGURE 4: Peptide mapping of Cys400 GA after treatment with DTT (A) and the fully oxidized Cys400 GA, obtained by bromobutyric acid/KI treatment, without DTT treatment (B). The GA derivatives were digested with endoproteinase Lys-C and subjected to reverse-phase HPLC on a Nucleosil C18 column at 45 °C. Nonlinear gradients were applied to effect the separation of the peptides. Insets: MALDI MS analysis of the Thr379−Lys404 peptide (arrows) following its deglycosylation by PNGaseF treatment. The calculated average mass for the deglycosylated Thr379−Lys404 peptide is 2767 Da. The broad peak at around 32 min does not give rise to a mass spectrum and most likely represents a nonpeptide impurity.

and was only obtained after DTT treatment of the digest. This may have involved reduction of the sulfenic acid of Cys400 (Cys400-SOH) (*37*) or a disulfide-linked form to the free thiol form. The second form of Thr379−Lys404 obtained represented a mass increase of 32 Da and was obtained in peptide maps from reaction products of treated Cys400 GA. It represents the sulfinic acid state of oxidation, Cys-SO_2H. The identification of the peptide was confirmed by C-terminal sequencing with carboxypeptidase Y, which resulted in sequential removal of Lys, Asp, and Tyr in accordance with the primary structure (*13*). The proportion

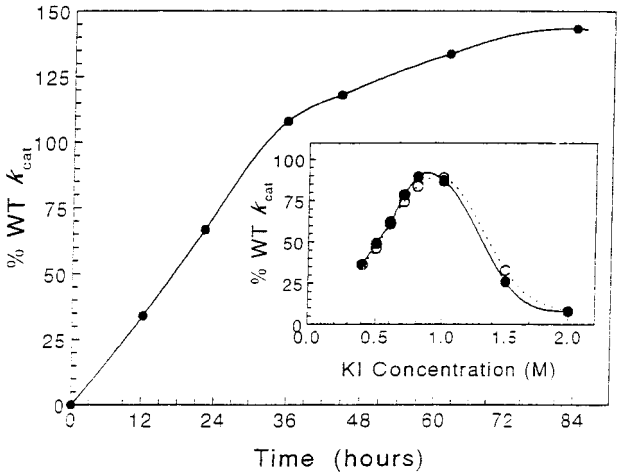

FIGURE 5: Regeneration of activity of Cys400 GA by oxidation with KI/Br_2. Cys400 GA (3.1 μM) in 0.2 M sodium acetate buffer, pH 5.1, was treated with 0.8 M KI and 10 μM Br_2 at 22 °C. At the times indicated, 25 μL samples of the reaction mixture were removed and assayed for activity against 30 mM maltose (saturating conditions) at 45 °C and expressed as a percentage of wild-type GA activity. Inset: Relationship between KI concentration and regeneration of Cys400 GA activity. Enzyme (3.1 μM) in the same buffer was treated with 0.4−2.0 M KI in the presence of 20 μM Br_2. Following 24 h (○) and 36 h (●) incubation at 22 °C, the percentage of wild-type activity against 30 mM maltose was assessed.

of this oxidized peptide in the Cys400 GA derivatives obtained with iodoacetic and iodopropanoic acid increased from approximately 30% to 60% of the total amount of peptide, reflecting the corresponding increase in restored activities (Table 2) of the two GA derivatives. In a final attempt to achieve the alkylation, Cys400 GA was treated in 6 M GdnHCl at pH 4.5 or 7.6 with 0.1−0.3 M iodopropionic acid. However, no alkylation of Cys400 resulted as determined by peptide mapping and MALDI MS analysis (data not shown), while, as found before, Cys400 was oxidized when the treatment was conducted at the low pH.

Oxidation of Cys400 GA. The data presented above strongly indicated that oxidation of Cys400 to Cys400-SO_2H had occurred via a side reaction during the alkylation experiments and was responsible for the dramatic increase by up to around 700-fold of the low catalytic activity of Cys400 GA, i.e., beyond the wild-type level. Preliminary experiments to specifically achieve this oxidation involved treatment of Cys400 GA with 0.02−0.1 M KI at pH 4.5 for 1−4 h at 22 °C. These reactions resulted in only minor activity increases and partial oxidation of Cys400 as determined by peptide mapping coupled with MALDI MS analysis (data not shown). These reactions with KI alone could not be controlled, and after a transient gain in activity, inactivation dominated which was probably caused by iodination of aromatic residues (*36*). Hence, conditions were established to gently oxidize Cys400 GA in a manner analogous to the treatment of the enzyme with 4-bromobutyric acid which had led to 160% activity relative to wild-type GA. Reaction of 3.1 μM Cys400 GA in 0.2 M sodium acetate buffer, pH 5.1, with a combination of KI and Br_2 did restore activity. This recovery of activity was found to be dependent upon KI concentration (Figure 5, inset), and 0.8 M KI was established to be optimum. The oxidation required at least 1 molar equiv of Br_2 relative to enzyme concentration for complete oxidation, while concentrations in excess of 30-fold were observed to prevent the full recovery of catalytic activity. As judged by the gain in activity, the optimum conditions established for the oxidation of 3.1 μM Cys400 GA at pH 5.1 involved 0.8 M KI in the presence of 10 μM Br_2 (Figure 5).

A semipreparative scale oxidation of Cys400 GA was conducted (see Materials and Methods) to provide enough material for subsequent characterization. Reaction of 3 nmol of the oxidized Cys400 GA in Tris·HCl, pH 7.8, with Ellman's reagent in the presence of 6 M GdnHCl did not lead to an increase in the absorbance at 412 nm, indicating the absence of a free thiol in this GA derivative. The loss of free thiol groups (Figure 3) when not accompanied by maximum gain in activity may arise from the initial conversion to the cysteinesulfenic acid, Cys400-SOH, which subsequently undergoes further oxidation to Cys400-SO_2H (*38*, *39*), present in the highly enzymatically active derivative of GA.

MALDI MS peptide mapping confirmed the oxidation of Cys400 in the GA derivative. The peptide Thr379−Lys 404 was isolated by RP-HPLC from both untreated and oxidized Cys400 GA following their digestion with endoproteinase Lys-C. The identity of the isolated peptide was confirmed by C-terminal sequencing.

Repeated MALDI MS analysis of each peptide after prior digestion with PNGase F to liberate the N-linked carbohydrate chain revealed a mass increase of 31−32 Da for the peptide obtained from the oxidized enzyme compared to that obtained from untreated Cys400 GA (Figure 4, insets). These data thus confirm that the direct oxidation, like the haloalkylcarboxylic acid treatments, resulted in the conversion of the Cys400 thiol to the sulfinic acid state. All peaks in the HPLC chromatogram in the vicinity of that containing the oxidized peptide were checked by MALDI MS prior to and after treatment with DTT. None of these contained the form with the free thiol group, indicating that the oxidation was complete.

Enzymic Activity of Cys400-SO_2H GA. As with Cys400 GA treated with bromobutyric acid, the k_{cat} of the KI/Br_2 oxidized derivative of Cys400 GA, Cys400-SO_2H GA, was approximately 700-fold greater than that of Cys400 GA with either maltose or maltoheptaose as substrate (Table 2). Likewise, Cys400-SO_2H GA acting on these substrates was characterized by higher k_{cat} values relative to wild-type GA. Whereas Cys400-SO_2H, Cys400, and wild-type GAs have similar K_m values for maltose, the K_m for the oxidized derivative was 3−4-fold increased toward maltoheptaose compared to wild-type GA. This suggested that favorable enzyme−substrate interaction(s) was (were) lost in the binding cleft beyond subsites −1 and +1 in Glu400 → Cys GA which, in contrast to the rate of hydrolysis, were not restored by oxidation (*40*).

IEF of Cys400-SO_2H GA. Under the conditions employed, IEF of Cys400-SO_2H GA gave a p*I* of 4.0 which was identical to both wild-type GA (*41*) and Cys400 GA. This lack of change in p*I* for the oxidized Cys400 GA derivative is in contrast to the observations with *p*-hydroxybenzoate hydroxylase where a decrease in p*I* of 0.4 pH unit for the sulfinic acid derivative compared to the unoxidized wild-type enzyme was noted (*39*). With GA, however, the

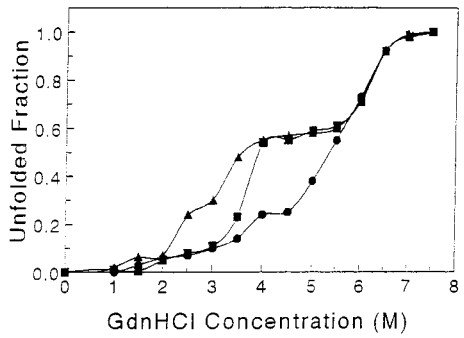

FIGURE 6: Denaturation by increasing concentration of GdnHCl for wild-type (●), Cys400 (▲), and Cys400-SO_2H (■) GAs.

relatively high number of acidic amino acid residues naturally present in the enzyme that generate its low p*I* likely mask the presence of the sulfinic acid in Cys400-SO_2H GA.

Stability of Cys400 GA and Cys400-SO_2H GA. Substitution of Glu400 by cysteine drastically reduced the thermostability of the enzyme. Thus, the T_{50} value of Cys400 GA was decreased by 19 °C to 53.5 °C, compared to T_{50} of 72.5 °C for wild-type GA (*25*). Oxidation of Cys400 slightly improved T_{50} to 59 °C for Cys400-SO_2H GA. Similarily, increased stability in GdnHCl was obtained through oxidation of Cys400 GA compared to unmodified Cys400 GA, although resistance to the chaotropic agent was far from fully restored to wild-type levels (Figure 6).

DISCUSSION

Replacement of the catalytic base Glu400 by Cys reduced the activity (k_{cat}) of the *A. awamori* GA to 0.2% of the wild-type level, but despite structural changes imposed at the active site, subsequent oxidation of Cys400 to cysteinesulfinic acid fully restored the hydrolytic activity. In fact, Cys400-SO_2H GA, with the gap at the catalytic site estimated to be 1.2 Å larger than in the wild-type GA (Table 1; Figure 2B), exhibits 1.6-fold higher activity, perhaps a result of Cys-SO_2H being a stronger acid with a pK_a reported to be 1.5 (*42*). This observation was totally unexpected in view of other reports concerning replacement of catalytic Glu residues with Asp, a potential catalytic residue with similar side-chain length as cysteinesulfinic acid. For example, replacement of either the catalytic nucleophile Glu78 or the acid−base catalyst Glu172 of *Bacillus circulans* xylanase with Asp resulted in 0.04% and 0.16% residual activity, respectively (*6, 43*). Likewise, replacement of catalytic Glu residues in *B. pumilus* xylanase (*44*) and *Agrobacterium* β-glucosidase (*45*) with Asp produced dramatic losses in activity. It is pertinent to mention, however, that each of these examples involves a retaining enzyme which follows a double-displacement mechanism of action (Figure 1) (*1*). No examples appear to exist in the literature regarding a similar Glu→Asp replacement of a catalytic base residue in an inverting enzyme.

There are two possible explanations that could account for the increase in activity noted for Cys400-SO_2H GA. First, another acidic residue positioned appropriately might assume the role of the catalytic base. This situation would be analogous to the change of an inverting to a retaining mechanism engineered in T4 phage lysozyme (*46*). In that study, a nucleophilic residue (Thr26→His) was introduced in the proximity of the nucleophilic water, that attacks at C-1 of substrate, without removal of the original catalytic base, Asp20. On first consideration, this possibility would seem unlikely for the present GA Glu400→Cys mutant because it has very low activity and inspection of its pH−activity profile (*40*) reveals the lack of an essential titratable group with a pK_a suitable of a catalytic base. Whereas oxidation of Cys400 could perturb the active site conformation to present another suitable amino acid residue in the vicinity of the catalytic center, this circumstance would seem remote given the apparent relatively large distance to the nearest acidic residue, Asp55, which in the crystal structure (*22*) would have to shift approximately 8 Å. Having excluded this possibility, it would appear that the introduced side chain cysteinesulfinylate group in Cys400-SO_2H GA does indeed act as the catalytic base.

To our knowledge, this is the first report of a combined site-directed mutagenesis−chemical modification approach to enhance the enzymatic properties of a specific catalytic residue. Applications of this approach have to date (*47* and references cited therein) followed the lead made with carboxypeptidase Y (*48*) by replacing and modifying residues either within binding clefts or elsewhere in the enzymes. Moreover, this is the first report of a cysteinesulfinic acid participating in the mechanism of action of an enzyme. Naturally occurring cysteinesulfenic acid has been identified at the catalytic center of enterococcal NADH peroxidase (*49*) and NADH oxidase (*50*), and this particular oxidation state of an active site Cys has been generated in a variety of other enzymes to modify their catalytic activities (reviewed in *50*), but nothing has been reported on the enhancement of activity by the introduction of a cysteinesulfinic acid residue. In addition, none of these enzymes are a glycosyl hydrolase. With Cys400-SO_2H GA, we presume that the putative increase in the gap between the catalytic residues is more than compensated for by the strengthening of the acidic properties of the general base catalyst.

Haloalkylcarboxylic acids are routinely used for the facile alkylation of cysteinyl residues in proteins, and so it was quite surprising that such a modification was not achieved with Cys400 GA, even at high reagent concentrations (0.1−0.2 M). Fortuitiously, however, it was the high reagent concentrations used in the current study that provided sufficient quantities of free halogen to catalyze the side-reaction oxidation of Cys400. One possibility for the lack of alkylation of the free sulfhydryl group by the various haloalkylcarboxylic acids could be that the active site pocket is lined with four acidic residues, Asp55, Asp176, Glu179, Glu180 (*18*), thereby producing a highly anionic environment which would likely repulse any entering exogenous acids. Future attempts to alkylate Cys400 will therefore involve various esters of haloalkylcarboxylic acids followed by mild-base hydrolysis to provide a new acidic moiety at Cys400.

The present study shows that a catalytic base is critical for efficient hydrolytic activity by this inverting enzyme. The mutation of the catalytic base Glu400 to Cys reduced the k_{cat} to 0.2% of wild-type whereas Glu400→Gln GA, as shown previously (*24*), has around 2% of the wild-type activity. This unusually high activity of Glu400→Gln GA was interpreted to indicate that in the wild-type GA, Glu400 is a weak base catalyst; the activity of the Glu400→Gln GA was thus reduced because of loss of electrostatic stabilization of the oxocarbenium ion intermediate, while the nucleophilic

Wat500 was able to react rapidly, even without assistance of the catalytic base (*24*). The finding that the activity of Cys400 GA is only 10% of Glu400→Gln GA in fact further supports the active role played by the Gln400 residue in the catalysis. Another difference is that whereas no great destabilization of the folded protein occurred in Glu400→Gln GA, T_{50} being lowered only by 4 °C relative to wild-type (*24*), the decrease in T_{50} by 19 °C for Cys400 GA reflects a very important decrease in conformational stability, probably caused by loss of hydrogen-bond network contacts at the active site. In wild-type GA, Glu400 is thus hydrogen-bonded to Tyr48, Ser411, Gln401, and Wat500; the latter in turn forms a hydrogen bond to Asp55 (*18*, *22*−*24*). This network is destroyed in Cys400 GA, but probably maintained in Glu400→Gln GA, as earlier deduced from the crystal structure (*24*). As Cys400-SO_2H GA has slightly higher thermostability and is somewhat more resistant to GdnHCl denaturation than Cys400 GA, reintroduction of an acidic side chain may have restored part of the hydrogen-bond network, albeit much less efficiently as present in wild-type or Glu400→Gln GAs.

The present study furthermore suggests that the position of the catalytic base is surprisingly flexible in this inverting enzyme. The restoration of hydrolytic activity to 160% of the wild-type level is in sharp contrast to the required precise positioning of the catalytic nucleophile in a retaining enzyme, e.g., xylanase from *Bacillus circulans* (*6*). This may be taken as an illustration of the different roles that the nucleophile and catalytic base play in retaining and inverting mechanisms, respectively (Figure 1). In the case of the retaining enzymes, the nucleophile has to be in contact with substrate to which it ultimately forms a covalent linkage (*2*, *4*, *6*). With inverting enzymes, the catalytic residue simply serves as general base, that abstracts a proton from water which subsequently directly attacks C-1 of the oxocarbenium ion intermediate (*51*). The fact that the generated hydroxide anion is thus free to migrate to C-1 presumably allows for some spatial flexibility of the catalytic base. It is also conceivable that considerable flexibility of the solvent structure in inverting carbohydrases permits accommodation of the shorter chain length of an engineered catalytic group without a major change of the catalytic site geometry. In this context, it is interesting to note that the putative catalytic groups observed in the recently reported three-dimensional structure of the inverting cellulase from *Clostridium thermocellum*, CelA (*52*), are only 5.8 Å apart, whereas the gap between the catalytic carboxyl groups observed in the crystal structures of most inverting enzymes is about 9 Å. To accommodate both a water molecule and substrate, the gap in CelA would have to open. Indeed, this strongly supports our conclusion that variation may exist for the location of the catalytic base in inverting glycosyl hydrolases.

It is pertinent to mention that the predicted distance between the catalytic residues Glu179 and Cys400-SO_2H noted above for Cys400-SO_2H GA is based upon static computer-generated models. The conformational flexibility of the active site may lead to unpredictable variations in the intercatalytic group distances. This may be further complicated by the expected change in enzyme conformation upon complexation of the GA derivative with substrate. Calculation of a structural model using energy minimizations was not attempted here because application of this technique to the Tyr48→Trp GA mutant previously failed to provide the same structure as that subsequently obtained by X-ray crystallography (*24*; B. B. Stoffer, personal communication). Nevertheless, given the apparent tight constraints observed within the active site of GA complexed with inhibitor (*22*), we are confident that the distance between the catalytic groups is increased in Cys400-SO_2H GA compared to wild-type GA.

Our results suggest that the inverting mechanism in *A. awamori* GA is very flexible in terms of accommodation of the catalytic base position. Oxidation of catalytic base Cys mutants in other inverting glycosyl hydrolases would be of interest to compare with the present results and to elucidate if the structural variation possible in GA is a general property of the inverting mechanism. Moreover, new insights in the catalytic mechanism of glycosyl hydrolases could be obtained by extending this approach to pursue replacement by a cysteine at the general acid, alone or together with the catalytic base, and subsequent oxidation. By applying such a strategy, the catalytic and enzymatic properties of the enzyme derivatives may be significantly improved. As shown in the following article (*40*), a detailed enzymatic characterization of this GA derivative indicated that the oxidation of the catalytic base Cys400 mutant also influenced the substrate specificity and the ability to catalyze the condensation reaction.

ACKNOWLEDGMENT

We are grateful to S. Ehlers for excellent technical assistance. Dr. I. Svendsen, B. Corneliussen, and L. Sørensen are acknowledged for N-terminal sequencing and amino acid analysis. We are indebted to Dr. T. P. Frandsen for help with Figures 1 and 2 and Table 1, and to Drs. M. Meldal and D. Tull for valuable discussions.

REFERENCES

1. Koshland, D. E. (1953) *Biol. Rev. 28*, 416−436.
2. McCarter, J., and Withers, S. G. (1994) *Curr. Opin. Struct. Biol. 4*, 885−892.
3. Davies, G., and Henrissat, B. (1995) *Structure 3*, 853−859.
4. Tull, D., Miao, S., Withers, S. G., and Aebersold, R. (1995) *Anal. Biochem. 224*, 509−514.
5. White, A., Tull, D., Johns, K., Withers, S. G., and Rose, D. R. (1996) *Nat. Struct. Biol. 3*, 149−154.
6. Lawson, S. L., Wakarchuk, W. W., and Withers, S. G. (1996) *Biochemistry 35*, 10110−10118.
7. Sierks, M. R., Ford, C., Reilly, P. J., and Svensson, B. (1989) *Protein Eng. 2*, 621−625.
8. Meagher, M. M., Nikolov, Z. V., and Reilly P. J. (1989) *Biotechnol. Bioeng. 34*, 681−688.
9. Fierobe, H.-P., Stoffer, B. B., Frandsen, T. P., and Svensson B. (1996) *Biochemistry 35*, 8696−8704.
10. Hiromi, K. (1970) *Biochem. Biophys. Res. Commun. 40*, 1−6.
11. Sierks, M. R., Ford, C., Reilly, P. J., and Svensson, B. (1990) *Protein Eng. 3*, 193−198.
12. Davies, G., Wilson, K. S., and Henrissat, B. (1997) *Biochem. J. 321*, 557−559.
13. Svensson, B., Larsen, K., Svendsen, I., and Boel, E. (1983) *Carlsberg Res. Commun. 48*, 529−544.
14. Svensson, B., Larsen, K., and Gunnarsson, A. (1986) *Eur. J. Biochem. 154*, 497−502.
15. Svensson, B., Jespersen, H., Sierks, M. R., and MacGregor, A. (1989) *Biochem. J. 264*, 309−311
16. Williamson, G., Belshaw, N. J., and Williamson, M. P. (1992) *Biochem. J. 282*, 423−428.

17. Stoffer, B., Frandsen, T. P., Busk, P. K., Schneider, P., Svendsen, I., and Svensson, B. (1993) *Biochem. J. 292*, 197−202.
18. Aleshin, A., Golubev, A., Firsov, L. M., and Honzatko, R. B. (1992) *J. Biol. Chem. 267*, 19291−19298.
19. Henrissat, B., Coutinho, P. M., and Reilly, P. J. (1994) *Protein Eng. 7*, 1281−1282.
20. Stoffer, B. (1994) Ph.D. Thesis, University of Copenhagen, Faculty of Science, Denmark.
21. Harris, E. M. S., Aleshin, A., Firsov, L. M., and Honzatko, R. B. (1993) *Biochemistry 32*, 1618−1626.
22. Aleshin, A. E., Firsov, L. M., and Honzatko, R. B. (1994) *J. Biol. Chem. 269*, 15631−15639.
23. Stoffer, B., Aleshin, A. E., Firsov, L. M., Svensson, B., and Honzatko, R. B. (1995) *FEBS Lett. 358*, 57−61.
24. Frandsen, T. P., Dupont, C., Lehmbeck, J., Stoffer, B., Sierks, M. R., Honzatko, R. B., and Svensson, B. (1994) *Biochemistry 33*, 13808−13816.
25. Fierobe, H.-P., Mirgorodskaya, E., Frandsen, T. P., Roepstorff, P., and Svensson B. (1997) *Protein Expression Purif. 9*, 159−170.
26. Clarke, A. J., and Svensson, B. (1984) *Carlsberg Res. Commun. 49*, 559−566.
27. Clarke, A. J., and Svensson, B. (1984) *Carlsberg Res. Commun. 49*, 111−122.
28. Bray, M. R., Carriere, A. D., and Clarke, A. J. (1994) *Anal. Biochem. 221*, 278−284.
29. Riddles, P. W., Blakeley, R. L.,and Zerner, B. (1983) *Methods Enzymol. 91*, 49−60.
30. Svensson, B., Larsen, K., and Svendsen, I. (1983) *Carlsberg Res. Commun. 48*, 517−527.
31. Karras, M., and Hillenkamp, F. (1988) *Anal. Biochem. 60*, 2299−2301.
32. Fox, J. D., and Robyt, J. F. (1991) *Anal. Biochem. 195*, 93−96.
33. Palcic, M., Skrydstrup, T., Bock, K., Le, N., and Lemieux, R. U. (1993) *Carbohydr. Res. 250*, 87−92.
34. Leatherbarrow, R. J. (1987) *Enzfitter, a nonlinear regression data analysis program for IBM PC*, Elsevier Science Publishers BV, Amsterdam, The Netherlands.
35. Frandsen, T. P., Christensen, T., Stoffer, B., Lehmbeck, J., Dupont, C., Honzatko, R. B., and Svensson, B. (1995) *Biochemistry 34*, 10162−10169.
36. Håkansson, K., and Svensson, B. (1989) *Carlsberg Res. Commun. 54*, 145−156.
37. Willett, W. S., and Copley, S. D. (1996) *Chem. Biol. 3*, 851−8567.
38. Allison, W. S. (1976) *Acc. Chem. Res. 9*, 293−299.
39. van Berkel, W. J. H., and Müller, F. (1987) *Eur. J. Biochem. 167*, 35−46.
40. Fierobe, H.-P., Clarke, A. J., Tull, D., and Svensson, B. (1998) *Biochemistry 37*, 3753−3759.
41. Svensson, B., Pedersen, T. G., Svendsen, I., Sakai, T., and Ottesen, M. (1982) *Carlsberg Res. Commun. 47*, 55−69.
42. Palmieri, F., Stipani, I., and Iacobazzi, V. (1979) *Biochim. Biophys. Acta 555*, 531−546.
43. Wakarchuk, W. W., Campbell, R. L., Sung, W. L., Davoodi, J., and Yaguchi, M. (1994) *Protein Sci. 3*, 467−475.
44. Ko, E. P., Akatsuka, H., Moriyama, H., Shinmyo, A., Hata, Y., Katube, Y., Urabe, I., and Okada, H. (1992) *Biochem. J. 288*, 117−121.
45. Withers, S. G., Rupitz, K., Trimbur, D., and Warren, R. A. J. (1992) *Biochemistry 31*, 9979−9985.
46. Kuroki, R., Weaver, L. H., and Matthews, B. W. (1995) *Nat. Struct. Biol. 2*, 1007−1011.
47. Berglund, P., DeSantis, G., Stabile, M. R., Shang, X., Gold, M., Bott, R. R., Graycar, T. P., Lau, C. M., and Jones, J. B. (1997) *J. Am. Chem. Soc. 119*, 5265−5266.
48. Bech, L. M., and Breddman, K. (1988) *Carlsberg Res. Commun. 53*, 381−393.
49. Yeh, J. I., Claiborne, A., and Hol, W. G. J. (1996) *Biochemistry 35*, 9951−9957.
50. Clairborne, A., Miller, H., Parsonage, D., and Ross, R. P. (1993) *FASEB J. 7*, 1483−1490.
51. Tanaka, Y., Tao, W., Blanchard, J. S., and Hehre, E. J. (1994) *J. Biol. Chem. 269*, 32306−32312.
52. Alzari, P. M., Souchon, H., and Dominguez, R. (1996) *Structure 4*, 265−275.

BI972231X